

On the fast transient spoiler deployment in a NACA0012 profile using LES techniques combined with AMR and IMB methods

F. Favre^{1,2}, O. Antepara¹, O. Lehmkuhl^{1,3}, R. Borrell³ and A. Oliva¹

¹ Heat and Mass Transfer Technological Center, Polytechnical University of Catalonia (UPC),
Colom 11, 08222, Terrassa, Barcelona, Spain. cttc@cttc.upc.edu

²Instituto de Ingeniería Mecánica y Producción Industrial, Universidad de la República del Uruguay
(UdelaR) Av. 18 de Julio 1968, 11300, Montevideo, Uruguay

³ Termo Fluids, S.L., Avda. Jaquard, 97 1-E, 08222 Terrassa (Barcelona), Spain

Key Words: *Adaptive mesh refinement; Large Eddy Simulations; Immersed Boundary.*

Abstract. Due to the high impact in final cost reduction, the development of active systems of load control for wind turbines has recently gained renewed interest. The use of these systems results in a faster and more detailed action over the blade's load than modern pitch-control systems, using aerodynamic control surfaces to locally modify the flux. Numerical simulations of these fluxes are presented in this work as a powerful tool for its understanding. A combination of large-eddy simulations (LES) techniques and the immersed-boundary method was employed in order to meet the conditions imposed by the mobile parts of the control systems embedded in the computational mesh. Use was also made of the Adaptive Mesh Refinement (AMR) method presented in [1] to minimize the amount of computational cells and therefore obtain an adequate resolution of the different length scales. A simulation of the experiment presented by Yeung et al. [2] was performed as a validation of the proposed model. The experiment consists of an aerodynamic profile deploying a control-surface with a $Re=3,5 \times 10^5$ flux.

1 INTRODUCTION

The control systems designed to alleviate blade fatigue damages in wind turbines have a huge impact in the kWh's final cost. For larger rotors this impact is even more critical. This, together with the recent increase in the size of rotors, has sparked interest in the development of a new generation of control system devices [3]. These new devices are developed to reduce the load fluctuations in blades in a fast and more localised way than current ones (modern pitch control, passive control, etc.) The more promising solutions incorporate mobile parts to the blades, namely, control surfaces, which react to wind changes modifying the profile's aerodynamics, thus enabling the force on the blade to be influenced.

The control-surface's study covers several topics such as materials, control-systems and aerodynamics. This work focuses in the last one, i.e., in the understanding of the control-surface's influence on the flux surrounding the blade. A number of experimental studies in wind tunnels and numerical simulations have been performed with this purpose, where simplified models of potential flux [4] and RANS model [5,6] have been used. In the present work we propose the application of more advanced models, such as LES. Given the unsteady shedding nature of these fluxes, better solutions are expected with this model.

A combination of large-eddy simulation (LES) techniques and the immersed-boundary

method (IMB) is proposed. A body conformal grid can be used to simulate fluxes around objects, and if these objects are moving independently, the grid has to dynamically change in time. Conversely, with the IMB method non-body conformal and static grids can be used. This, in combination with the adaptive mesh refinement (AMR), allows to minimise the computational cells, have a good spatial resolution in the objects location, and adequately describe the different length scales of the flux. These methods are further described in Section 2.

A numerical simulation of the experiment presented in [2] is performed employing the above-mentioned methods. Results are presented in Section 3. The case consists of a flux around a NACA-0012 profile with a null angle of attack and Reynolds number of 3.5×10^5 based on the profile chord (c). A spoiler located in the upper surface of the profile is deployed during the experiment. This case proves ideal for testing the here proposed methods because of the mobile component attached to an aerodynamic profile.

2 MATHEMATICAL AND NUMERICAL MODEL

The dimensionless governing equation in primitive variables of incompressible flows of Newtonian fluids are:

$$\frac{\partial u}{\partial t} + (u \cdot \nabla) u = \frac{1}{Re} \Delta u - \nabla p \quad (1)$$

$$\nabla \cdot u = 0 \quad (2)$$

In the present work, the turbulent flow is described by means of LES using symmetry-preserving discretizations. The spatial filtered and discretized Navier-Stokes equations can be written as,

$$M u = 0 \quad (3)$$

$$\Omega \frac{\partial \bar{u}}{\partial t} + C(\bar{u}) \bar{u} + \nu D \bar{u} + \rho^{-1} \Omega G \bar{p} = C(\bar{u}) \bar{u} - \overline{C(u) u} \approx -M T_m \quad (4)$$

where M , C , D and G are the divergence, convective, diffusive and gradient operators respectively, Ω is a diagonal matrix with the sizes of control volumes, ρ is the fluid density, ν is the viscosity, \bar{p} represents the filtered pressure, \bar{u} is the filtered velocity, M represents the divergence operator of a tensor, and T_m is the SGS stress tensor. The LES model used in the present work is the WALE model within a variational multiscale framework [7] (VMS-WALE). The spatial discretization preserves the symmetry properties of the continuous differential operator, ensure stability and conservation of the global kinetic energy on any grid [7-10].

The fractional-step method is employed to perform the time evolution of the equations. The convective and diffusive terms are explicitly treated with an Adams-Benshfort scheme.

$$\frac{\vec{u}_p - \vec{u}_n}{\Delta t} = \alpha_0 H(\vec{u}^n) + \alpha_1 H(\vec{u}^{n-1}) = RHS^n \quad (5)$$

$$G p^{n+1} = \frac{1}{\Delta t} M \bar{u}_p \quad (6)$$

$$\bar{u}_{n+1} = \bar{u}_p - \Delta t G p^{n+1} \quad (7)$$

The time integration method is summarized in equations 5,6 and 7, where H is a spatial operator containing convective and diffusive terms and \bar{u}_p is the predictor velocity.

2.1 IMB

The presence of objects immersed in the mesh is not taken into account in the model. However, this can be achieved by using the IMB method, which modifies the equations. A source term \vec{f} is added in momentum calculation

$$\frac{\vec{u}_p - \vec{u}_n}{\Delta t} = RHS^n + \vec{f} \quad (8)$$

The value of \vec{f} is calculated in such a way that the velocity in each node of the grid considers the presence of the object, therefore, f has a non-zero value only in those nodes which are inside the object, or are outside the object but because of their closeness they are influenced by it. This idea is used in a number of works [11-14]. To calculate f the following equation is used.

$$\vec{f} = \frac{\vec{V} - \vec{u}^n}{\Delta t} - RHS \quad (9)$$

When the movement of the object is known, the value of V of the interior points is directly calculated from their coordinates. However, for the forcing points some approximation has to be used because by definition these nodes are outside the object, according to Fadlun et al [11] using a second order interpolation to calculate V , the global accuracy of the scheme is maintained. In order to perform the interpolation for a forcing point, equation 10 is applied. Four velocities are used: one refers to the closest point of the object and the other three are velocities of exterior nodes which are neighbours of the forcing point.

$$\vec{V} = a_w \vec{u}_w + a_1 \vec{u}_{nb1} + a_2 \vec{u}_{nb2} + a_3 \vec{u}_{nb3} \quad (10)$$

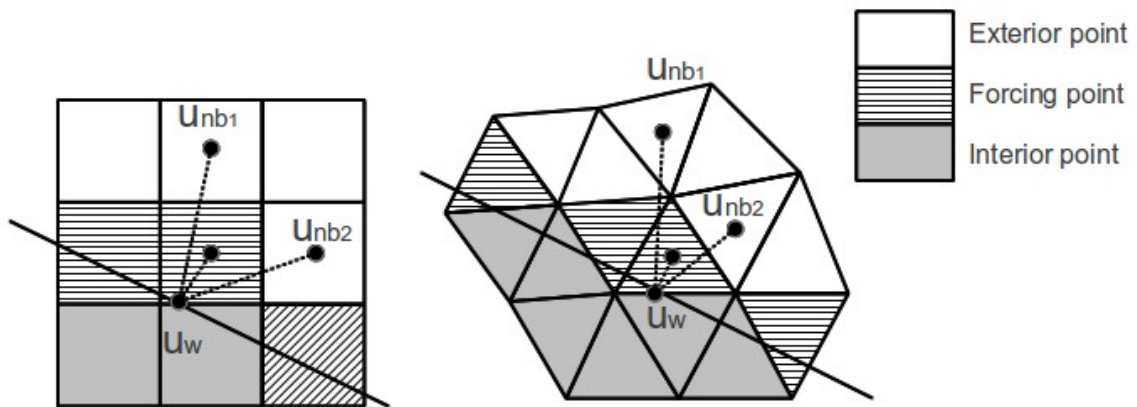


Figure 1: Example of Control Volumes intersected by an object.

To determine the coefficients' values only geometric data are needed, therefore, if the object is still they are calculated only once and stored, and if the object is moving they must be recalculated each iteration.

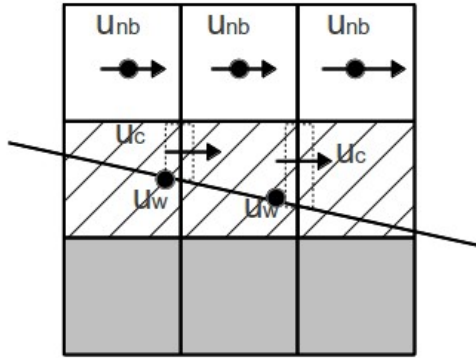


Figure 2: Diagram of predictor mass correction on Poisson Equation

Since linear interpolation is applied to the predictor velocity, an error is here made. This is due to the modification of the interpolated velocities in the projection step and the possible change in the linear relationship among velocities. To reduce this effect, the Poisson equation (6) is modified as described in [12] and [13]. This modification is an improvement of the idea introduced by Kim et al in [14], and consists of a more detailed calculation of the predictor flux in the faces intersected by the object, as is shown in Figure 2.

When a face is intersected by the object, two polygons are determined: one inside the object and another one outside the object. The outside polygon is hereafter considered the real face. The flux of m_{face}^p on this face is computed using the following expression,

$$m_{face}^p = A_c \vec{u}_c \vec{n} \quad (11)$$

where A_c is the surface of the polygon immersed in the fluid and \vec{u}_c is computed via a linear interpolation at the centroid of the polygon.

2.2 AMR

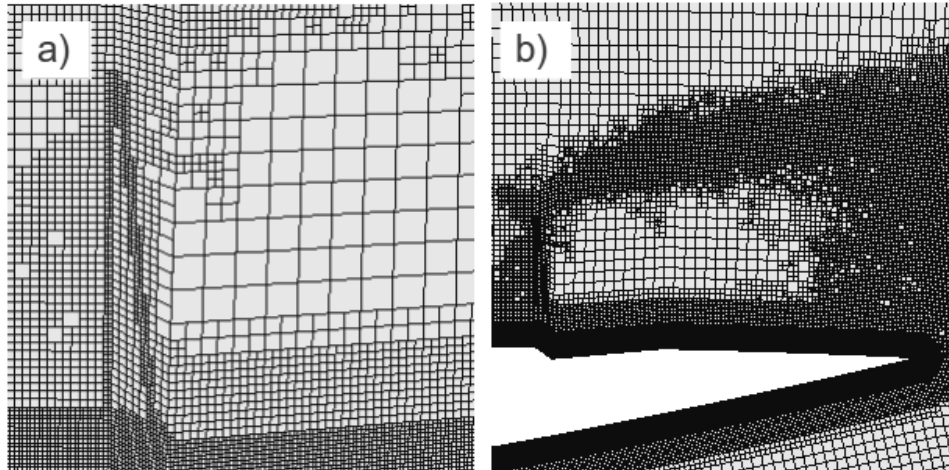


Figure 3: Computational domain. a) Refinement near the object. b) Refinement using physics criteria.

In order to minimize the number of computational cells, the methods presented before can be combined with AMR, a method presented in earlier works [1]. A parent cell is refined in four (2D refinement) children cells in the region where the resolution must be increased.

Conversely, the refinement can be reversed in over-resolved regions by coarsening, i.e., four children cells are combined in one parent cell.

The method is based on linear interpolations: the vertex coordinates of the parent cell are averaged to determine the new vertex of the children cells. Furthermore, a tree data structure is used in order to keep track of the computational cells and communicate information from the old mesh to the new one.

Two images of the mesh used in this work to validate the model are shown in Figure 3. Figure 3a) illustrates the improved spatial resolution obtained in the the object's region as a result of mesh refinement. Figure 3b) shows the refinement applied to regions where more resolution is needed for the flow to be adequately described. The criteria used for this case is based on our understanding of the physics of the case.

3 RESULTS

In order to validate the proposed method the experiment presented in [2] was simulated. Initially a flux around a NACA-0012 profile with a null angle of attack and Reynolds number of 3.5×10^5 based on c is computed. A spoiler is located on the upper surface of the profile between $0.7c$ and $0.8c$ -Figure 5 shows its geometry. After the flux is fully developed, the spoiler starts the deployment, rotating up to 90° with a motion given by equation 12. The axis of rotation is illustrated in Figure 6. In Figure 4 an instantaneous of the flow with the spoiler fully deployed is shown.

$$\beta(t) = \beta_i + (\beta_f - \beta_i) \frac{1}{2} \left(1 - \cos \left(\left(\frac{t - t_i}{t_f - t_i} \right) \pi \right) \right) \quad (12)$$

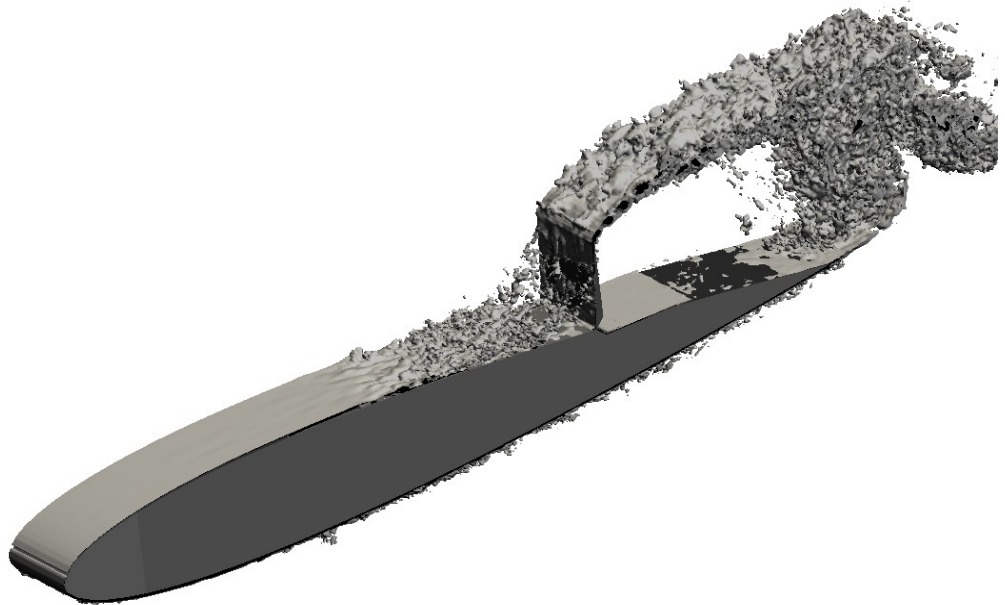


Figure 4: Vorticity contour surfaces with the spoiler fully deployed.

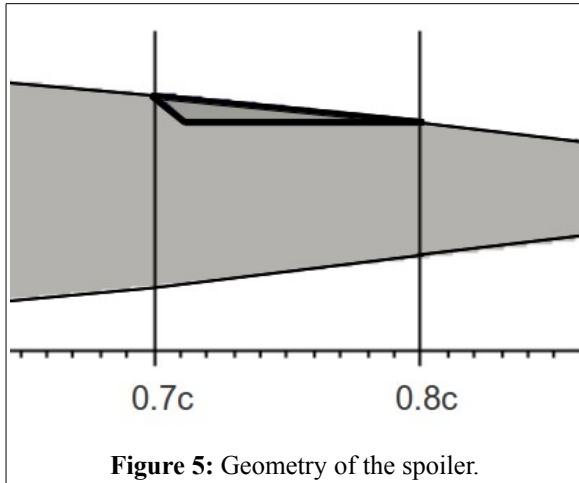


Figure 5: Geometry of the spoiler.

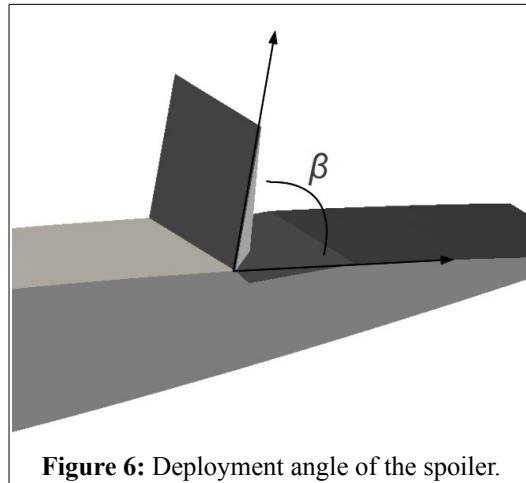


Figure 6: Deployment angle of the spoiler.

In Section 3.1 details of the grids employed to discretize space are presented and in Section 3.2 numerical results are showed and compared with the experimental results from Yeung et al.

2.2 Spatial discretization

Two kinds of grids were used: one body-fitted mesh (mesh A) comprised of quads which enable the use the AMR method, and an unstructured mesh constructed with triangles (mesh B). Both meshes were constructed conformal to the modified NACA-0012 geometry because of the presence of the spoiler, and extruded in the normal direction of the profile using 32 planes.

At the beginning of the simulation the total number of nodes in mesh A is 2.800.000. This number is increased by mesh refinement along the simulation due to:

(a) the need for an area refinement near the spoiler which increases when the bottom face of the spoiler is detached from the object (b) the new characteristics of the flux after its passage through the spoiler. Once the spoiler is completely deployed the total number of nodes stabilize around 4.400.000.

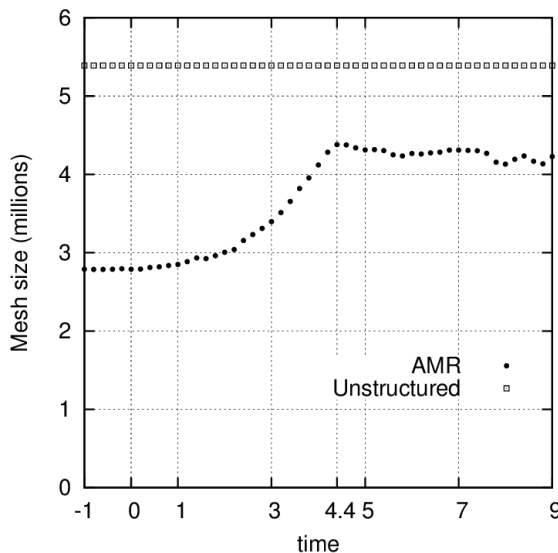


Figure 7: Number of computational cells along the simulation for both meshes.

In contrast, the total number of nodes in mesh B is fixed at 5.400.000 along the entire simulation. Note that at any given time there are more nodes in mesh B than in mesh A. This is because the static mesh has to be fine enough at any area and time needed for the calculations. Figure 7 shows a comparison of the total number of nodes of both meshes along the simulation.

2.2 Results

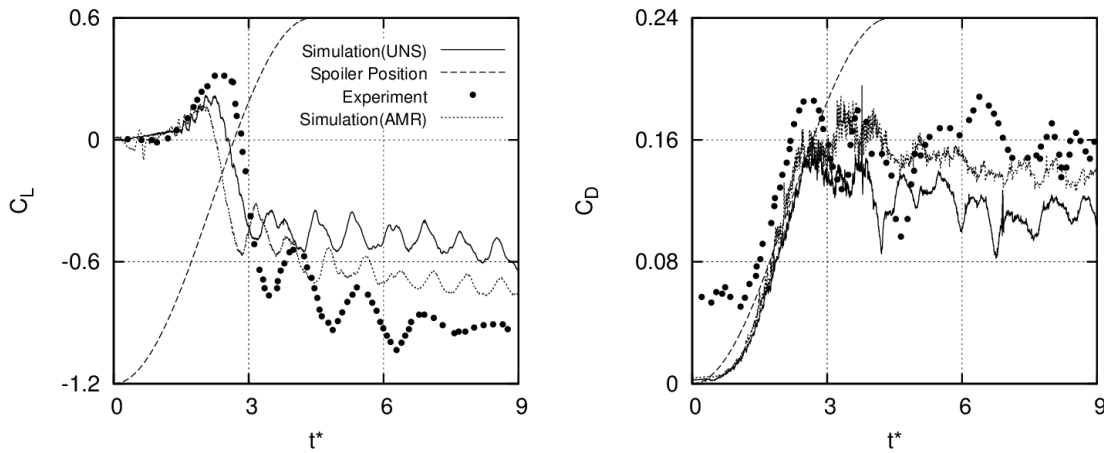


Figure 8: Numerical and experimental evolution of Lift and Drag.

The time evolution of the coefficients of Lift and Drag along the simulation are compared against the experimental values measured by Yeung et al. in their experiment and shown in Figure 8. The solution shows a reasonable agreement for both meshes.

The same flow characteristics are observed both in the simulation and the experiment, according to what was reported by Yeung et al. in [2]. Given the surface discontinuity originated in the beginning of the deployment at the tip of the spoiler, the flow is separated from it generating a strong vortex behind the spoiler. Therefore, a low pressure region is created and an initial increase of Lift is induced. However, since the purpose of placing the spoiler is to obtain a negative Lift, this is an adverse Lift.

As the vortex moves downstream, the pressure in that area still being low, the pressure under the profile decreases and that over the profile and before the spoiler increases. Consequently, the Lift starts to reduce. In the experiment this

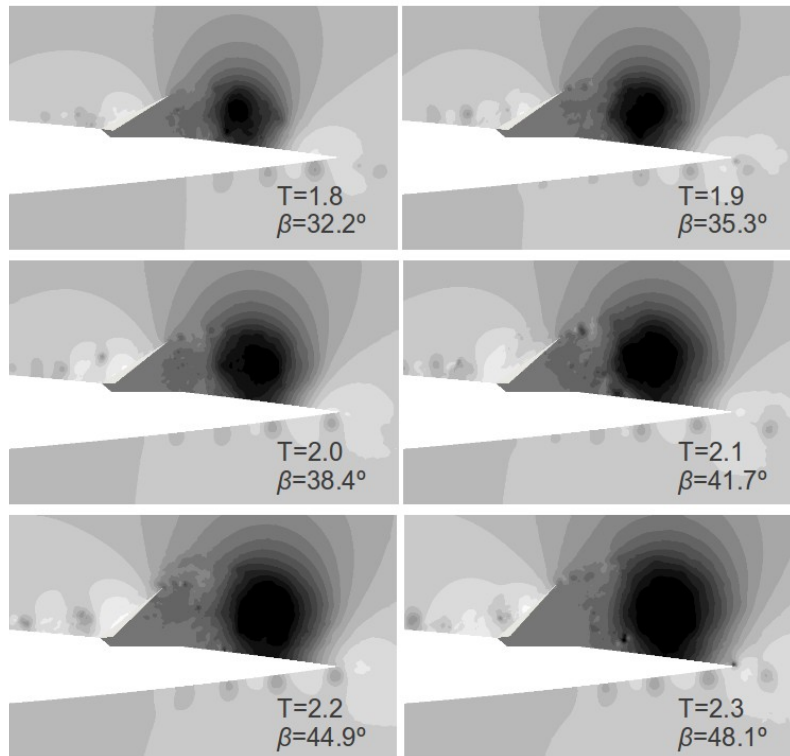


Figure 9: Pressure contour plot near the spoiler around lift's peak time (mesh A).

occurs at $2.27 s^*$, while in the simulation this happens earlier, at $2.14s^*$ for mesh B and at $2.03s^*$ for mesh A. The time evolution of this vortex can be observed with the pressure fields show in Figure 9.

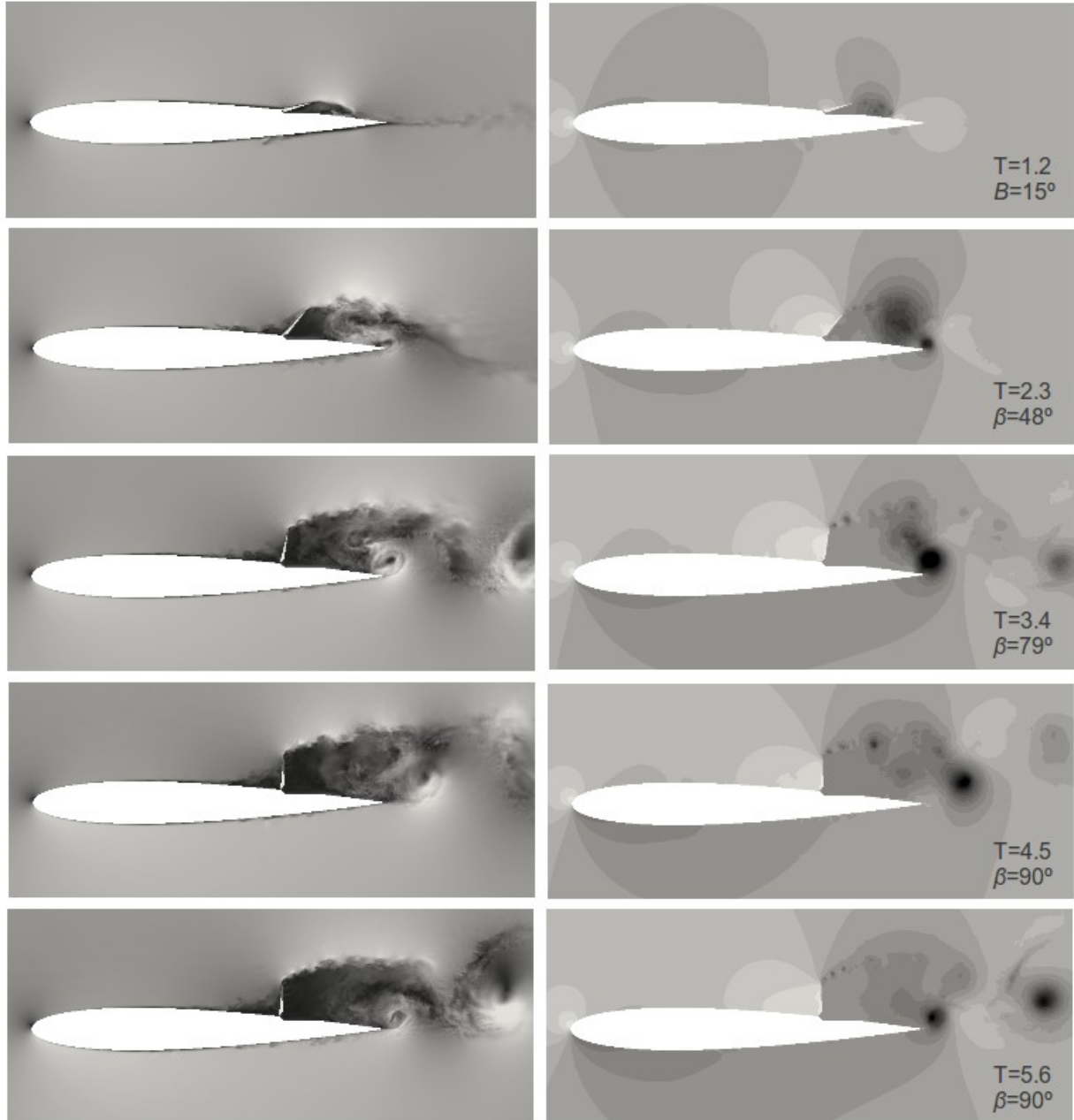


Figure 10: Instantaneous velocity fields (left) and pressure contour plots (right) during the spoiler deployment (mesh A).

When the spoiler is completely deployed, the flow continues separating from its tip. This flow interacts with the shear layer formed in the trailing edge, so periodic vortex shedding in

the wake take place. Finally Lift and Drag oscillate around a stable value, which is well reproduced by the simulation, having better results for the mesh A, for which the AMR method is employed.

Figure 10 shows pressure and vorticity fields for different times during the spoiler deployment.

4 CONCLUSIONS

A combination of LES techniques and the IMB method shows to be a potent tool in the study of new solutions to the problem of load control on wind turbines. It was shown that these methods can be easily combined with AMR in order to reduce the computational cost of the simulations.

It is possible to simulate flows around industrial profiles including diferents control surfaces in a 2D and a half conditions using the implemented method, in order to study the transitory response of new devices. Moreover, 3D simulations can be conducted because of the characteristics of the methods, therefore an entire blade can be simulated with independent control surfaces along it.

ACKNOWLEDGMENTS

This work has been financially supported by the Ministerio de Economía y Competitividad, Secretaría de Estado de Investigación, Desarrollo e Innovación, Spain (ENE2010-17801), and by TermoFluids S.L. Additionally F. Favre wishes to thank the Agencia Nacional de Investigación e Innovación (ANII), Uruguay, for its financial support in the form of a doctoral degree scholarship.

REFERENCES

- [1] O. Antepara, O. Lehmkuhl, J. Chiva, R. Borrell. *Parallel Adaptive Mesh Refinement Simulation of the Flow Around a Square Cylinder at $Re = 22000$* 25th International Conference on Parallel Computational Fluid Dynamics. 61:246–250, (2013).
- [2] Yeung W. W. H; Xu C; Gu W. *Reduction of Transient Adverse Effects of Spoilers*. Journal of Aircraft, Vol 34, No. 4, July-August, pp. 478-484, (1997).
- [3] T.K. Barlas, G.A.M. Van Kuik. *Review of state of the art in smart rotor control research for wind turbines*. Progress in Aerospace Sciences 46 1-27 (2010).
- [4] T. Buhl, C. Bak, M. Gaunaa and P. B. Andersen, *Load Alleviation throught adaptive Trailing Edge Control Surfaces. ADAPWING Overview*. Scientific proceedings. Brussels : European Wind Energy Association (EWEA), (2007).
- [5] R. Chow and C.P. Van Dam. *On the temporal response of active load control devices*. Wind Energy 13:135-149 (2010).
- [6] Trodlborg, N., *Computational Study of the RisØ-B1-18 Airfoil Equipped with Actively Controlled Trailing Edge Flaps*”, Master Thesis, Technical University of Denmark, Department of Mechanical Engineering, Fluid Mechanics, (2004).
- [7] O. Lehmkuhl, I. Rodríguez, A. Baez, A. Oliva, C.D. Pérez-Segarra, *On the large-eddy simulations for the flow around aerodynamic profiles using unstructured grids*, Computers & Fluids, 84:176-189, (2013).

- [8] I. Rodríguez, O. Lehmkuhl, R. Borrell, A. Oliva, *Direct numerical simulation of a NACA0012 in full stall*, International Journal of Heat and Fluid Flow 43: 194-203, (2013).
- [9] T.J.R. Hughes, L. Mazzei and K.E. Jansen. *Large eddy simulation and the variational multiscale method*. Computing and Visualization in Science 3: 47–59, (2000).
- [10] R. W. C. P. Verstappen and A. E. P. Veldman. *Symmetry-Preserving Discretization of Turbulent Flow*. Journal of Computational Physics 187: 343–368, (2003).
- [11] Fadlun EA, Verzicco R, Orlandi P, Mohd-Yusof J. *Combined Immersed-Boundary finite-difference methods for three-dimensional complex flow simulations*. J Computational Physics 161(1):35-60, (2000).
- [12] Wei-Xi Huang and Hyung Jin Sung. *Improvement of mass source/sink for an immersed boundary method*. International Journal for Numerical Methods in Fluids 53:1659-1671 (2007).
- [13] S. Kang, G. Iaccariono and P. Moin, *Accurate Immersed-Boundary Reconstructions for Viscous Flow Simulations*. AIAA Journal Vol 47, No7 (2009).
- [14] Kim, Kim and Choi. *An immersed-boundary finite-volume method for simulation of flow in complex geometries*. Journal Of Computational Physics 160:705-719, (2001).